Journal of
Physics
Students

http://www.jphysstu.org

X-Ray and Infrared Studies for $NiSi_XFe_{2-x}O_4$ Ferrites

D. M. Hemeda*, M. Z. Said

Physics Department, Faculty of Science, Tanta University, Egypt
**: Corresponding Author: dahemeda@yahoo.com*

Received 24 September 2007; accepted 10 January 2008

Abstract - A spinel ferrite of the system $NiSi_xFe_{2-x}O_4$ with (x = 0, 0.1, 0.2, 0.3, 0.4 and 0.5) were studied via IR, X-ray spectra and cation distribution. The X-ray pattern confirmed the spinel cubic structure of all Si contents. The lattice parameters estimated as a function of Si contents indicated a slight decrease of lattice parameter up to 0.2. The grain size increases with increasing Si content up to 0.3 and then decreases for higher Si content. The jump length of electrons decreased with Si concentration up to 0.2. Four absorption bands were observed in infrared spectra in the range between 1000 and 200 cm^{-1}. These bands are assigned to Fe^{3+} and Si^{4+} at the A- and B-sites. The two high frequency bands in the range 580-555 and 450-400 cm^{-1} is assigned to υ_1 tetrahedral (A-site) and υ_2 octahedral (B-site).

Keywords: X-ray, Ferrite, IR, cation distribution, grain size.

1. Introduction

Ferrimagnetic oxides, ferrite, crystallizes with two magnetic sub-lattice, tetrahedral A-site and octahedral B-site. The electrical and magnetic properties, upon which its application depends, depend on the distribution of cations among these sites. Nickel ferrite and Zn^{2+} doped nickel ferrites are widely used in electronics and electrical industries as they exhibit interesting variation in electrical and magnetic properties. Ni occupies the octahedral B-site; Zn^{2+} occupies tetrahedral A-site and Fe^{3+} is distributed between tetrahedral and octahedral sites. By increasing Zn^{2+} concentration, the Fe^{3+} ions at A-sites decrease while the Fe^{3+} ions at B-sites increase causing the total magnetic moment to increase [1-6].

Far infrared spectra of the ferrite samples in the range 1000-200 cm^{-1} were reported elsewhere [7-11]. Four bands were observed, the high frequency band υ_1 is assigned to tetrahedral complexes, a small band υ_2 is due to divalent metal oxygen complexes at B-sites and υ_3 is assigned to the lattice vibration of the system. The splitting occurred in the υ_1 and υ_2 bands is due to the presence of Fe^{2+} ions in the tetrahedral and octahedral sites. However, no information exists in the literature regarding the structural IR spectra, X-ray and the jump length of electrons of Si doped Ni-ferrite. Therefore, in this paper, X-ray and IR spectra of $NiSi_xFe_{2-x}O_4$ system are reported.

2. Experimental Procedure

Composition of $NiSi_xFe_{2-x}O_4$ (x = 0, 0.1, 0.2, 0.3, 0.4 and 0.5) polycrystalline ferrites were prepared by standard ceramic preparation technique by using AR grad oxides NiO, Si and Fe_2O_3 wherein double sintering is employed. Composites were pre-sintered in a furnace at 900 ^oC in the presence of air for 24 hours and then let to cool at room temperature. Final sintering was carried out at 1200 ^oC for 6 hours [9-11].

The X-ray diffraction pattern for each sample was recorded using Shimadau X-Ray Diffractometer (Model XD-3). The powder specimens were exposed to CuK_α radiation. The IR spectra were recorded using Perkin Elmer IR Spectrometer Model 1430.

3. Results and Discussion

3.1. Crystallographic:

X-ray diffraction patterns for $NiSi_xFe_{2-x}O_4$ ferrite are shown in Fig. (1). The recorded reflection planes (220), (311), (222), (400), (422), (511), (440) and (622) which proved the formation of single phase of spinel cubic.

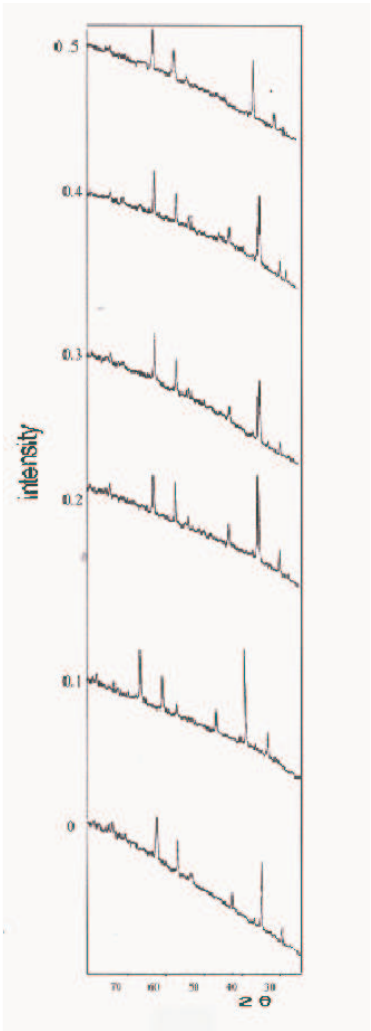

Fig. 1. X-ray diffraction pattern of $NiSi_xFe_{2-x}O_4$ with x = 0, 0.1, 0.2, 0.3, 0.4 and 0.5.

3.2. Effect of Si content on the lattice parameter:

The lattice parameter, a, is estimated for all Si content using the equation [12]

$$A = d_{hk\ell} (h^2 + k^2 + \ell^2)^{1/2} \quad (1)$$

where d is the interatomic distance. The effect of Si concentration on the lattice parameter is illustrated in Fig. (2). It is observed that the lattice parameter, a, decreased with enhancing Si content. This is attributed to the replacement of Si^{4+} (0.042 Å) of smaller size to Fe^{3+} ions (0.64 Å) of larger size at A- and B-sites. The behavior of these results is similar to that in previous work [13].

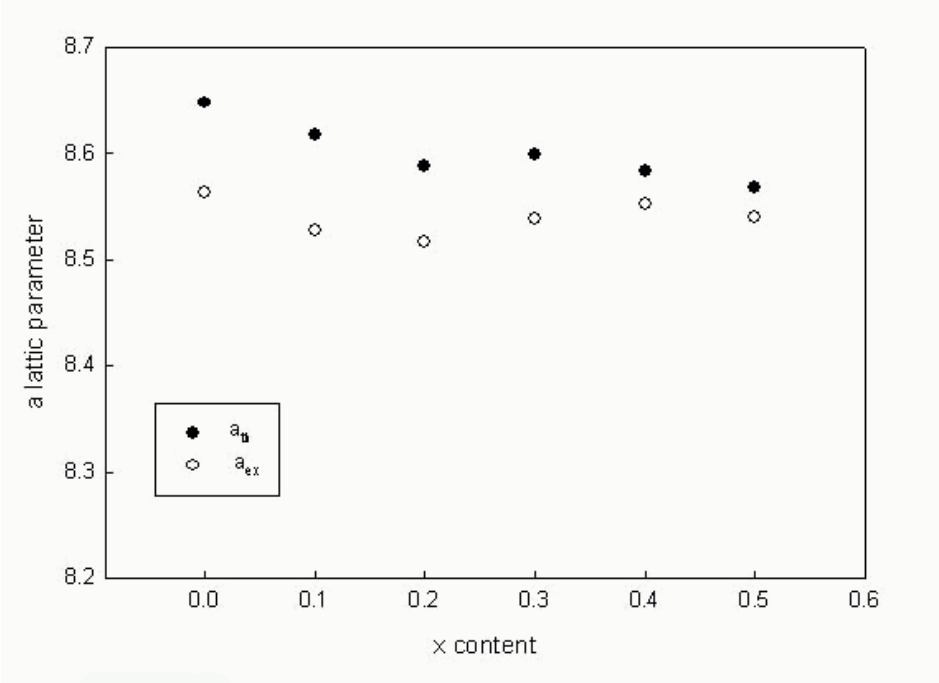

Fig. 2. The lattice parameters experimental and theoretical as a function of Si content.

3.3. Grain size:

Figure (3) shows the average grain size $\overline{D}$ as a function of Si content. It is observed that the average grain size increases with Si content. The grain size is in proportional to the line width for diffraction peaks. The average grain size is calculated using the Scherer equation (2) [14]

$$\overline{D} = \frac{K\lambda}{h_{1/2}\cos\theta} \quad (2)$$

where K = 51.57 is the Scherer constant, λ = 1.5405 Å is the wavelength of the CuK_α radiation, $h_{1/2}$ is the peak width at half maximum and θ corresponds to the peak positions. The volume distribution showed that the particle size range from 210-240 Å for Si concentration. All the grain sizes were within the spinel limits [12]. The increase of the grain size with increasing Si concentration up to 0.3 might be due to the substitution of Si ions for Fe^{3+} ions in the lattice. This is not accompanied by the generation of charged vacancies. It is believed that the doping ions concentrated near the grain boundaries [15-16]. The grain boundary motions will increase, since the lighter Si ions replace the relatively heavy iron ions. Also, Si

ions have smaller atomic volume than iron ions do, larger ionic displacements in the lattice will be more probable. This leads to the observed increase in the grain size. For Si content greater than 0.3, charged vacancies are therefore generated and are still bounded to the impurity ions because of their opposite charges. Some locations act as precipitating centers for Si ions at grain boundaries. These large locations decrease the number of mobile dislocations, thus reduce the mobility of grain boundaries leading to reduction of grain size.

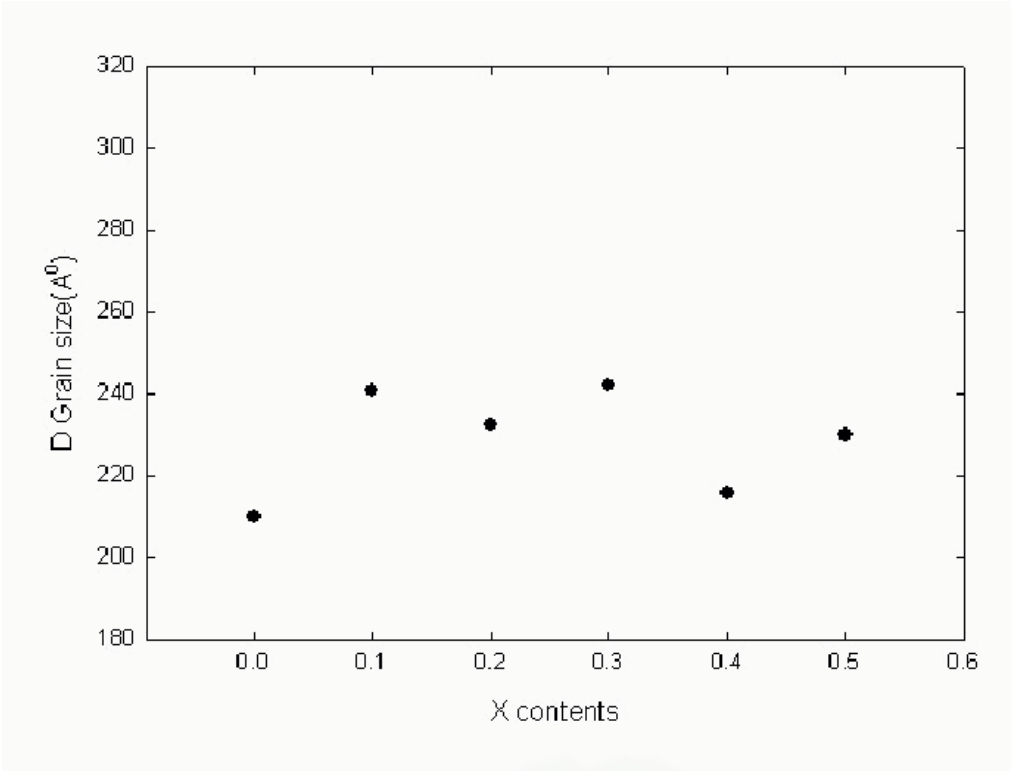

Fig. 3. The average grain size $\overline{D}$ as a function of Si content.

3.4. Effect of silicon concentration x on the jump length in $NiSi_xFe_{2-x}O_4$:

The jump length, L, of electrons is determined from equation (3) [17]:

$$L = a \frac{\sqrt{2}}{4} \qquad (3)$$

where a is the lattice parameter. The lattice parameters are determined from the observed values of X-ray diffraction pattern and so the B-B interaction responsible for conduction increases. The existence of strong B-B exchange interaction between ions on the B-sites of such a ferrite will affect the jump length of electrons between Fe^{2+} and Fe^{3+}. The jump length has a predominant role in explaining the behaviour of conductivity in the ferrite compositions. The effect of Si addition on the jump length is shown in Fig. (4). The addition of Si ions, which occupy A- and B-sites, leads to replacement of Fe^{3+} ions. The only conduction mechanism that can take place in this composition is the electron exchange interaction between Fe^{2+} and Fe^{3+} ions. Increasing silicon concentration results in a corresponding decrease in the ferrous ions which is responsible for electrical conduction. The nonmagnetic silicon ions replace the magnetic ferric ions and dilute the magnetization at the B-sites leading to decrease the jump with increasing Si content. This behaviour result is similar to previous work [18].

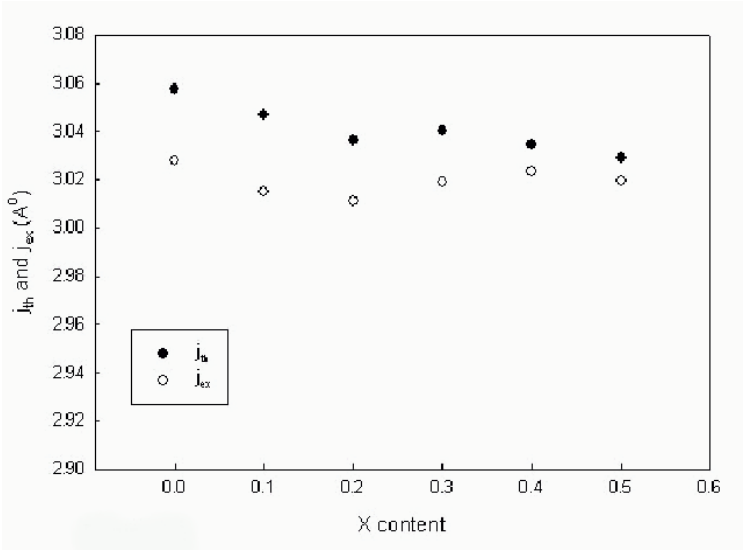

Fig. 4. The jump length experimental and theoretical as a function of Si content.

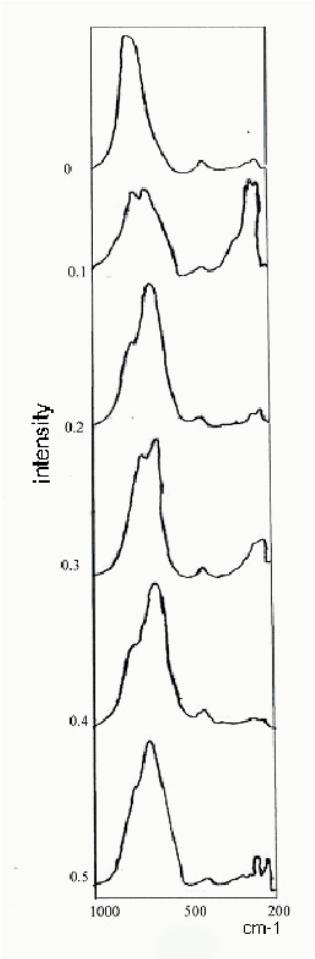

Fig. 5. IR spectra of $NiSi_xFe_{2-x}O_4$ system.

3.5. Infrared spectra:

Infrared spectral studies of $NiSi_xFe_{2-x}O_4$ system (x = 0, 0.1, 0.2, 0.3, 0.4 and 0.5) is shown in Fig. (5). The results of IR studies are listed in Table (1). The two strong absorption bands υ_1 and υ_2 are

observed and assigned to the complexes of Fe^{3+}-O^{2-} at the A-site and of Fe^{3+}-O^{2-} at the B-site mode of vibration [8-11]. The change in the band positions is due to the change in the Fe^{3+}-O^{2-} internuclear distances for the A- and B-sites. It is obvious that the bands υ_1 and υ_2 shift toward the high energy with enhancing Si^{4+} replacement for Fe^{3+} ions. The decrease of Fe^{3+} concentration at the A- and B-sites caused the increasing of the metal-oxygen stretching vibrational energies and reducing the size of the unit cell [9]. A new band $\upsilon_1^{'}$ in A-site is appeared in the IR around 790 cm^{-1} for x > 0 can be related to the stretching vibrational mode of Si^{4+}-O^{2-} tetrahedral [19]. On the octahedral site, the band $\upsilon_2^{'} \approx 380$ can be due to the presence of small fraction of Fe^{2+} ions in the samples [17,18]. Thus, $\upsilon_2^{'}$ can be attributed to Fe^{2+}-O^{2-} octahedral complexes. Besides, the four absorption bands there is another band around 270 cm^{-1} (υ^*) for x > 0 which may be due to the iron silicide (FeSi) [20].

Table 1. IR absorption data for $NiSi_xFe_{2-x}O_4$.

x	$\upsilon_1^{'}$ (cm^{-1})	υ_1 (cm^{-1})	υ_2 (cm^{-1})	$\upsilon_2^{'}$ (cm^{-1})	υ^* (cm^{-1})	υ_{th} (cm^{-1})	E (eV)
0	-	570	400	382	-	811	0.101
0.1	781	582	447	-	268	756	0.094
0.2	792	550	448	378	270	722	0.090
0.3	784	566	434	-	276	733	0.091
0.4	788.8	552	448	378	267	711	0.088
0.5	788.8	580	444	380	266	722	0.090

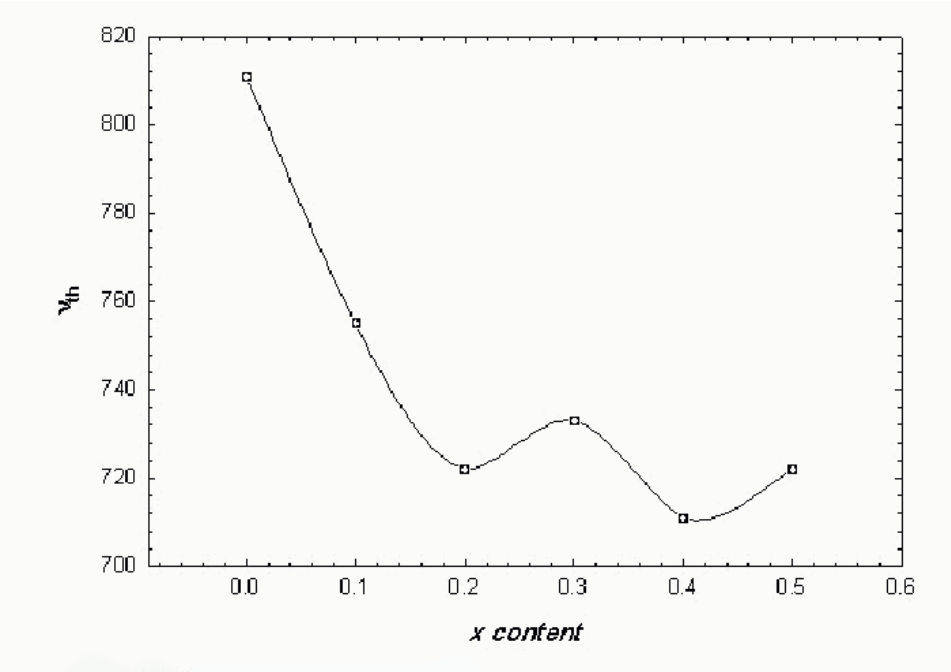

Fig. 6. The theoretical frequency, υ_{th}, as a function of Si content.

According to Waldron [7], the threshold frequency υ_{th} for the electronic transition can be determined from the maximum point of the absorption spectra. Figure (6) and Table (1) show these thresholds frequency values with Si content. It was found that the υ_{th} decreased by increasing the tetravalent content. The corresponding threshold energy was calculated (Table 1).

3.6. Effect of Si concentration on the intensity of IR absorption:

Figure (7) illustrates the effect of Si concentrations on the intensity of absorbed bands at the A- and B-sites. It is obvious that the intensity increases with enhancing Si content. This is attributed to the substitution of Si^{4+} ion to Fe^{3+} ion at A- and B-sites. The smaller size of Si^{4+} than that of Fe^{3+} causes the decrease of the bond length of Fe^{3+}-O^{2-} giving rise to the stretching force. This force needs higher absorbed intensity to permit for the bond Fe^{3+}-O^{2-} to be oscillated under the influence of IR waves. The increase of the intensity of absorption with enhancing impurity concentrations was previously studied on ferrite compositions [8,11]. This confirmed our interpretation.

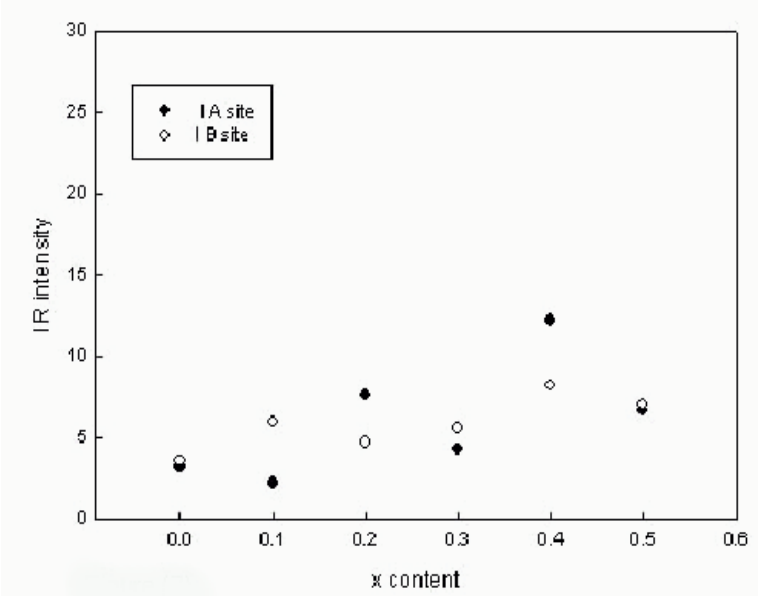

Fig. 7. The intensity of the IR absorption bands for both A- and B-sites as a function of Si content.

3.7. Band width:

The half band width of A- and B-sites in the IR spectra as a function of Si concentration is shown in Fig. (8). It is observed that the decrease of the half band width as the Si concentration is increased can be explained as follows:

Table 2. The cation distribution for $NiSi_xFe_{2-x}O_4$.

x	Cation distribution
0	$(Ni^{2+}_{0.1} + Fe^{3+}_{0.9})\,[Ni^{2+}_{0.9} + Fe^{3+}_{1.1}]$
0.1	$(Ni^{2+}_{0.1} + Si^{4+}_{0.0382} + Fe^{3+}_{0.8618})\,[Ni^{2+}_{0.9} + Si^{4+}_{0.0618} + Fe^{3+}_{1.0382}]$
0.2	$(Ni^{2+}_{0.1} + Si^{4+}_{0.0382} + Fe^{3+}_{0.8618})\,[Ni^{2+}_{0.9} + Si^{4+}_{0.1618} + Fe^{3+}_{0.9382}]$
0.3	$(Ni^{2+}_{0.1} + Si^{4+}_{0.0382} + Fe^{3+}_{0.8618})\,[Ni^{2+}_{0.9} + Si^{4+}_{0.2618} + Fe^{3+}_{0.8382}]$
0.4	$(Ni^{2+}_{0.1} + Si^{4+}_{0.0382} + Fe^{2+}_{0.0382} + Fe^{3+}_{0.8236})\,[Ni^{2+}_{0.9} + Si^{4+}_{0.3618} + Fe^{2+}_{0.3618} + Fe^{3+}_{0.3764}]$
0.5	$(Ni^{2+}_{0.1} + Si^{4+}_{0.0382} + Fe^{2+}_{0.0382} + Fe^{3+}_{0.8236})\,[Ni^{2+}_{0.9} + Si^{4+}_{0.4618} + Fe^{2+}_{0.4618} + Fe^{3+}_{0.1764}]$

The half band width depends on the statistical distribution of the various cations on the A- and B-sites [21]. This distribution depends on the replacement of Si^{4+} of smaller size to Fe^{3+} of larger size. Si^{4+}-O^{2-} represents a dominant role in retarding the oscillation of these bands at the A- and B-sites and control the width of the absorbed band. The ratios of the band width at B-sites to that at A-sites limit the amount of Si^{4+} which replaces the Fe^{3+} at A- and B-sites. On the basis of the half band width, one can suggest qualitatively the cation distribution (Table 2).Also if the ferric ions are partly replaced by one of the tetravalent ions the valency of an equal part of ferric ions is lowered by one. This is shown in table (2) [22]. It is known that there is a correlation between the ionic radius and the lattice parameter, so it can be calculated theoretically by the following equation [23]:

$$a_{th} = \frac{8}{3\sqrt{3}} [(r_A + R_o) + \sqrt{3} (r_B + R_o)] \quad (4)$$

where R_o is the radius of oxygen ion (0.14 nm), r_A and r_B are the ionic radii of tetrahedral and octahedral sites respectively.

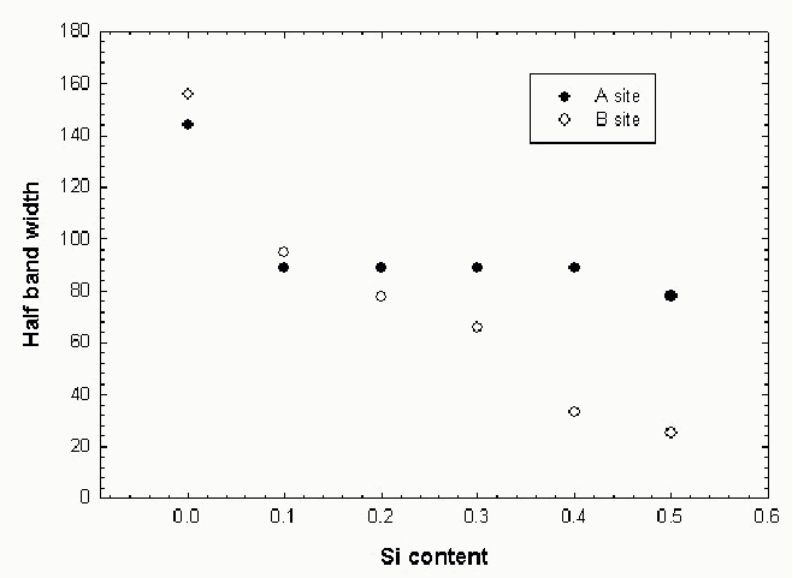

Fig. 8. The half band width of A- and B-sites as a function of Si-content.

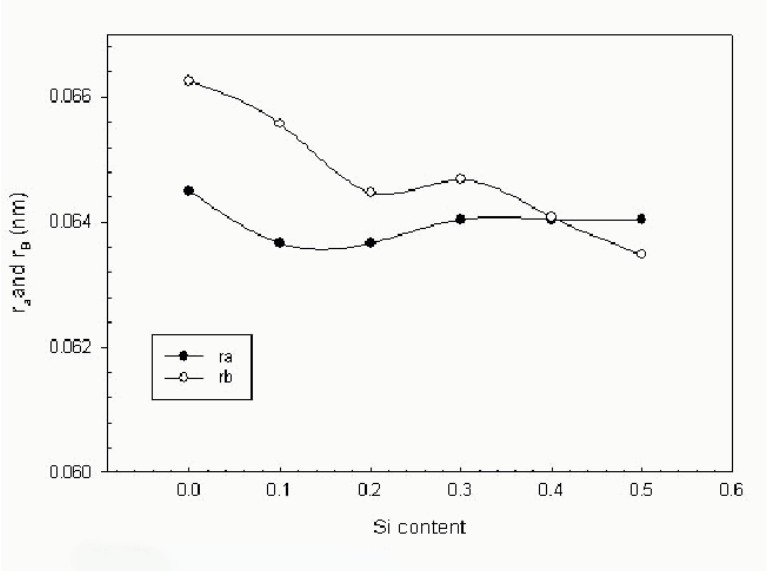

Fig. 9. r_A and r_B as a function of Si content.

We can use the cation distribution estimated from infrared analysis to calculate r_A and r_B. The theoretical and experimental lattice parameter values are plotted against Si^{4+} concentration in Fig. (2). It is noted that a_{th} is greater than a-experimental .The r_A and r_B which depend on the assumption of the cation distribution are plotted versus Si^{4+} content as shown in Fig. (9). It was seen that r_A decreased and remains constant for $x > 0$ but for r_B it decreased with Si content as discussed before.

4. Conclusion

X-ray analyses have demonstrated the spinel structure of the studied system. The substitutions of Si^{4+} ions to Fe^{3+} ions decrease the lattice parameter with increasing Si content. The grain size increases up to Si content < 0.3 and then decreases for higher concentrations. This is due to precipitation of Si^{4+} ion on the grain boundary which causes retarding of grain boundary mobility. The jump length of electrons decreases which retard mobility of electrons for conduction. This caused by the substitution of nonmagnetic Si^{4+} ions to magnetic Fe^{3+} ions which weakened the magnetization at B-sites. The IR spectra of the studied systems describe the shift of the absorbed bands to higher frequency with Si content. This is because the substitution of Si^{4+} to Fe^{3+} changes the bond length Fe^{3+}-O^{2-}. The r_A and r_B and a_{th} were calculated from the cation distribution which was estimate from IR spectra. It was found that the Si^{4+} enter in both A-site and B-site.

References

[1] B.V. Bhise, M.B. Dongare, S.A. Patil and S.R. Sawant, J. Mater. Sci. Lett. **10**, 922 (1991).
[2] A.R. Das, V.S. Anathan and D.S. Khan, J. Appl. Phys. **57**, 4149 (1985).
[3] S. Geller, J. Appl. Phys. **37**, 1408 (1966).
[4] S.A. Mazen, A.A. Yousif and M.E. Elzain, Phys. Stat. Sol. (a), **149**, 685 (1985).
[5] S.A. Mazen, A.H. Wakif and S.A. Mansour, J. Mater. Sci. **31**, 2661 (1996).
[6] M.C. Sable, B.K. Labde and N.R. Shamkuwar, Bull. Mater. Sci. **28**(1), 35 (2005).
[7] R.D. Waldron, Phys. Rev. **99**, 1727 (1955).
[8] M.A. Amer and O.M. Hemeda, Hyperfine Inter. **96**, 99 (1995).
[9] M.A. Amer, Phys. Stat. Sol. (a), **151**, 205 (1995).
[10] M.A. Amer, Phys. Stat. Sol. (a), **145**, 157 (1994).
[11] O.M. Hemeda and M.I. Abd El-Ati, J. Mag. and Magnet. Mater. **51**, 42 (2001).
[12] O.M. Hemeda, Turk. J. Phys. **28**, 121 (2004).
[13] G.A. Gaballa, A.I. El-Shora, M.A. Henaish and S.A. El-Attar, Phase Trans. **46**, (1994)67.
[14] G.K. Joshi, A.Y. Khot and C.R. Swagnt, Solid State Comm. **65**(12), 1593 (1988).
[15] R.B. Atkin and R.M. Futrath, J. Amer. Ceram. Soc. **54**(5), 265 (1971).
[16] A. Tawfik, A.I. Eatah and F. Abd El-Salam, Mater. Sci. Eng. **60,** 145 (1983).
[17] B. Gillot, F. Jemmali, Phys. Stat. Sol. (a), **765** (1983).
[18] A. Tawfik and S.A. Olofa, J. Mag. and Magnet. Mater. **174**, 133 (1997).
[19] S.A. Mazen, J. Mater. Chem. Phys. **62**, 131 (2001).
[20] M. Nikolaeva, M. Sendova-Vassileva, D. Dimova -Malinovska, D. Karpuzou, J.C. Pivin and G. Beshkou, Vacuum, **69**, 221 (2002).
[21] S.A. Mazen, M.H. Abdallah, B.A. Sabrah and H.A.M. Hashem, Phys. Stat. Sol. (a), **134**, 263 (1992).
[22] E.W.Gorter. Saturation Magnetization and crystal chemistry of ferromagnetic oxides. Philips Res. Rep.**9**(1954)295.
[23] O.M.Hemeda ,M.Z.Said ,M.M.Barakat J. Mag. and Magnet. Mater.**224**(2001)132-142